Dual Manifold Adversarial Robustness:
Defense against L_p and non-L_p Adversarial Attacks

Wei-An Lin[*][†]
University of Maryland
walin@umd.edu

Chun Pong Lau[*]
Johns Hopkins University
clau13@jhu.edu

Alexander Levine
University of Maryland
alevine0@cs.umd.edu

Rama Chellappa
Johns Hopkins University
rchella4@jhu.edu

Soheil Feizi
University of Maryland
sfeizi@cs.umd.edu

Abstract

Adversarial training is a popular defense strategy against attack threat models with bounded L_p norms. However, it often degrades the model performance on normal images and more importantly, the defense does not generalize well to novel attacks. Given the success of deep generative models such as GANs and VAEs in characterizing (approximately) the underlying manifold of images, we investigate whether or not the aforementioned deficiencies of adversarial training can be remedied by exploiting the underlying manifold information. To partially answer this question, we consider the scenario when the manifold information of the underlying data is available. We use a subset of ImageNet natural images where an approximate underlying manifold is learned using StyleGAN. We also construct an "On-Manifold ImageNet" (OM-ImageNet) dataset by projecting the ImageNet samples onto the learned manifold. For this dataset, the underlying manifold information is exact. Using OM-ImageNet, we first show that adversarial training in the latent space of images (i.e. on-manifold adversarial training) improves both standard accuracy and robustness to on-manifold attacks. However, since no out-of-manifold perturbations are realized, the defense can be broken by L_p adversarial attacks. We further propose *Dual Manifold Adversarial Training (DMAT)* where adversarial perturbations in both latent and image spaces are used in robustifying the model. Our DMAT improves performance on normal images, and achieves comparable robustness to the standard adversarial training against L_p attacks. In addition, we observe that models defended by DMAT achieve improved robustness against novel attacks which manipulate images by global color shifts or various types of image filtering. Interestingly, similar improvements are also achieved when the defended models are tested on (out-of-manifold) natural images. These results demonstrate the potential benefits of using manifold information (exactly or approximately) in enhancing robustness of deep learning models against various types of novel adversarial attacks. Codes and models will be available in this link.

1 Introduction

Deep neural networks have achieved impressive success in several fields including computer vision, speech, and robot control [1, 2, 3]. However, they are vulnerable against *adversarial attacks* [4, 5, 6, 7,

---

[*]First two authors contributed equally.
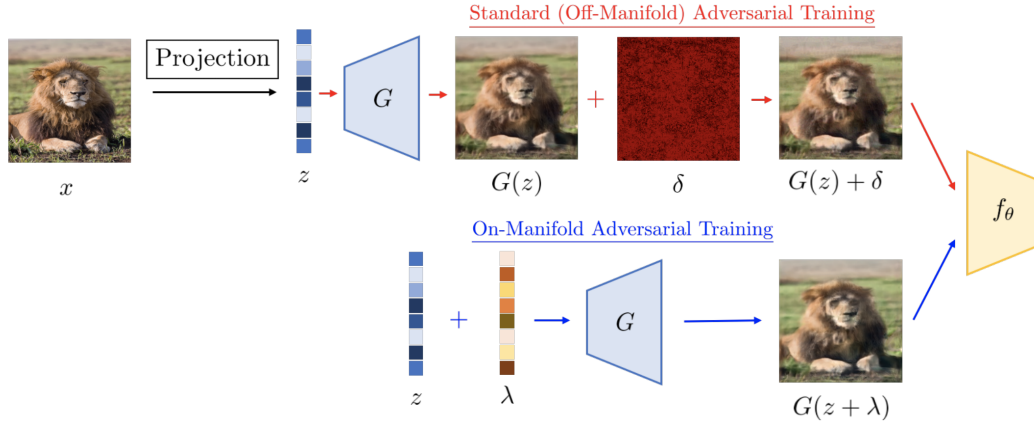
[†]Wei-An Lin is now at Adobe.

Figure 1: The overall pipeline of the proposed Dual Manifold Adversarial Training (DMAT). In this paper, we consider the scenario when the information about the image manifold is available. This is achieved by projecting natural images x onto the range space of a trained generative model G. We empirically show that either standard adversarial training or on-manifold adversarial training alone does not provide sufficient robustness, while DMAT achieves improved robustness against unseen attacks. During test time, images are directly passed to the adversarially trained classifier.

8, 9] which add, often imperceptible, manipulations to inputs to mislead the model. Sensitivity against adversarial attacks poses a huge challenge in security-critical applications where these networks are used. To improve the robustness of deep neural networks against different adversarial threat models, several empirical and certifiable defense methods have been proposed in the past few years including empirical defenses [10, 11, 12, 13], certifiable defenses [14, 15, 16, 17, 18, 19] and defences that detect and reject adversarial examples [20, 21, 22].

Among all of these defenses, *Adversarial training* (AT) [23], which augments the training data with adversarial examples, is perhaps the most standard one. Most existing AT methods consider adversarial distortions within a small L_p ball, and demonstrate robustness to the same type of distortion. However, robustness to L_p distortions often comes with the cost of reduced standard accuracy [24]. Moreover, models trained solely on L_p attacks are shown to generalize poorly to unforeseen attacks and are vulnerable to imperceptible color shifts [25], image filtering [26], and adversarial examples on the data manifold [27, 28]. Being robust against unseen attacks is critical in practice since adversaries will not follow a particular attack threat model.

Existing defenses consider properties of the trained classifier while ignoring the particular structure of the underlying image distribution. Recent advances in GANs and VAEs [29, 30, 31] are shown to be successful in characterizing the underlying image manifold[3]. This motivates us to study whether or not leveraging the underlying manifold information can boost robustness of the model, in particular against unseen and novel adversarial attacks. Our key intuition is that, in many cases, the latent space of GANs and VAEs represent compressed semantic-level features of images. Thus, robustifying in the latent space may guide the classification model to use robust features instead of achieving high accuracy by exploiting non-robust features in the image space [32].

In this paper, we attempt to answer this question by considering the scenario when the manifold information of the underlying data is available. First, we construct an "On-Manifold ImageNet" (OM-ImageNet) dataset where all the samples lie *exactly* on a low-dimensional manifold. This is achieved by first training a StyleGAN on a subset of ImageNet natural images, and then projecting the samples onto the learned manifold. With this dataset, we show that an on-manifold adversarial training (i.e. adversarial training in the latent space) could *not* defend against standard off-manifold attacks and vice versa. This motivates us to propose **D**ual **M**anifold **A**dversarial **T**raining (**DMAT**), which mixes both off-manifold and on-manifold AT (see Figure 1). AT in the image space (i.e.

---
[3]We use the term "manifold" to refer to the existence of lower-dimensional representations for natural images. This is a commonly used term in the generative model area. However, this definition may not satisfy the exact condition of manifolds defined in mathematics.

off-manifold AT) helps improve the robustness of the model against L_p attacks while AT in the latent space (i.e. on-manifold AT) boosts the robustness of the model against unseen non-L_p attacks.

Over the OM-ImageNet, we empirically show that DMAT leads to comparable robustness with standard AT against L_∞ attacks. Moreover, DMAT significantly outperforms standard AT against novel L_p and non-L_p attacks. For example, *for unseen L_2 and Fog attacks, DMAT improves the accuracy by 10% compared to standard adversarial training*. Interestingly, similar improvements are also achieved when the defended models are evaluated on (out-of-manifold) natural images. These results shed some light on the use of the underlying manifold information of images to enhance the intrinsic robustness of the models, specially against novel adversarial attacks.

2 Preliminaries

Setup. We consider the classification task where the image samples $x \in \mathcal{X} := \mathbb{R}^{H \times W \times C}$ are drawn from an underlying distribution $\mathbb{P}_X$. Let f_θ be a parameterized model which maps any image in $\mathcal{X}$ to a discrete label y in $\mathcal{Y} := \{1, \cdots, |\mathcal{Y}|\}$. An *accurate* classifier maps an image x to its corresponding true label y_{true}, i.e. $f_\theta(x) = y_{\text{true}}$. Without loss of generality, we assume $\mathbb{P}_X$ is supported on a lower-dimensional manifold $\mathcal{M}$ and can be approximated by $\mathbb{P}_{G(Z)}$ where $G(\cdot)$ is a generative model and Z is distributed according to the normal distribution. Informally, we refer to the support of $G(Z)$ as the approximate image manifold $\bar{\mathcal{M}}$ for $\mathcal{M}$. We say the manifold information is *exact*, when there exists a generative model G such that $\mathcal{M} = \bar{\mathcal{M}}$.

Standard adversarial robustness. We say x_{adv} is an adversarial example of the input image x if $f_\theta(x) = y_{\text{true}}$, $f_\theta(x_{adv}) \neq y_{\text{true}}$, and the difference between x_{adv} and x are imperceptible[4]. Most existing works consider L_p additive attacks where $x_{adv} = x + \delta$ subject to $\|\delta\|_p < \epsilon$. Formally,

$$\max_{\delta \in \Delta} \mathcal{L}(f_\theta(x + \delta), y_{\text{true}}), \tag{1}$$

where $\Delta = \{\delta : \|\delta\|_p < \epsilon\}$ and $\mathcal{L}$ is a classification loss function (e.g. the cross-entropy loss). In this paper, we focus on $p = \infty$, and will explicitly specify the type of norm when $p \neq \infty$ is used. In (1), since the function is non-convex, the maximization is typically performed using gradient-based optimization methods. The Fast Gradient Sign Method (FGSM) [5] is an L_∞ attack which uses the sign of the gradient to craft adversarial examples:

$$\delta = \epsilon \cdot sign\left(\nabla_x \mathcal{L}(f_\theta(x), y_{\text{true}})\right). \tag{2}$$

The Projected Gradient Descent (PGD) [23] attack is an iterative version of FGSM, which applies K steps of gradient descent. In the rest of the paper, we will use the notation PGD-K to represent K-step PGD attacks with bounded L_∞ norm.

To defend against norm-bounded attacks, an established approach by Madry *et al.* [23] considers the following min-max formulation:

$$\min_\theta \sum_i \max_{\delta \in \Delta} \mathcal{L}(f_\theta(x_i + \delta), y_{\text{true}}), \tag{3}$$

where the classification model f_θ is trained exclusively on adversarial images by minimizing the cross-entropy loss. This approach is called adversarial training (AT). Notice that when the manifold information is exact, we have $x_i = G(z_i)$ for some z_i. Thus, the standard adversarial training can be expressed as:

$$\min_\theta \sum_i \max_{\delta \in \Delta} \mathcal{L}(f_\theta(G(z_i) + \delta), y_{\text{true}}). \tag{4}$$

On-manifold adversarial robustness. The concept of on-manifold adversarial examples has been proposed in prior works [33, 27, 34]. For any image $x_i \in \mathcal{M}$, we can find the corresponding sample $G(z_i)$ on $\bar{\mathcal{M}}$ which best approximate x_i, where $z_i = \arg\min_z \|G(z) - x_i\|_2$. Adversarial examples that lie on the manifold can then be crafted by manipulating the latent representation z_i.

$$\max_{\lambda \in \Lambda} \mathcal{L}(f_\theta(G(z_i + \lambda)), y_{\text{true}}), \tag{5}$$

where $\Lambda = \{\lambda : \|\lambda\|_\infty < \eta\}$. Similar to standard adversarial attacks in the image space, the maximization in (5) can be performed by FGSM or PGD-K, which we denote as OM-FGSM

---

[4]There are some perceptible adversarial attacks such as patch attacks that we do not consider in this paper.

and OM-PGD-K respectively. In [27], it has been shown that deep learning models trained by standard AT (3) can be fooled by on-manifold adversarial examples. To defend against on-manifold attacks, [34] considers a similar mini-max formulation in the latent space:

$$\min_{\theta} \sum_{i} \max_{\lambda \in \Lambda} \mathcal{L}(f_\theta(G(z_i + \lambda)), y_{\text{true}}). \tag{6}$$

This approach is called the on-manifold adversarial training (OM-AT). In [34], on-manifold adversarial training has been shown to improve generalization on datasets including EMNIST [35], Fashion-MNIST [36], and CelebA [37]. In [33], the authors finetune an adversarially trained model with on-manifold adversarial examples and demonstrate improved robustness on MNIST [38]. Results from these works are restricted to artificial images where only limited textures are present. However, it has been shown that the vulnerability of deep learning models actually results from the fact that the models tend to exploit non-robust features in natural images in order to achieve high classification accuracy [32]. Therefore, whether the manifold information can be used to enhance the robustness of deep learning models trained on natural images is underexplored.

Notations. To precisely specify adversarial training procedures, in the rest of the paper, we will add the attack threat model that an adversarial training algorithm uses. For example, "AT [PGD-5]" refers to the standard adversarial training algorithm (4) with the PGD-5 (L_∞) attack used during training, and "OM-AT [OM-FGSM]" refers to the on-manifold adversarial training algorithm (6) with OM-FGSM (L_∞) as the attack method used during training.

3 On-Manifold ImageNet

One major difficulty of investigating the potential benefit of manifold information in general cases is the inability to obtain such information exactly. For approximate manifolds, the effect of the distribution shift between $\mathcal{M}$ and $\bar{\mathcal{M}}$ is difficult to quantify, leading to inconclusive evaluations. To address the issue, we propose a novel dataset, called On-Manifold ImageNet (OM-ImageNet), which consists of images that lie exactly on-manifold.

Our OM-ImageNet is build upon the Mixed-10 dataset introduced in the `robustness` library [39], which consists of images from 10 superclasses of ImageNet. We manually select 69,480 image-label pairs as $\mathcal{D}_{tr}^o = \{(x_i, y_i)\}_{i=1}^{N}$ and another disjoint 7,200 image-label pairs as $\mathcal{D}_{te}^o = \{(x_j, y_j)\}_{j=1}^{M}$, both with balanced classes. We first train a StyleGAN [40] to characterize the underlying image manifold of $\mathcal{D}_{tr}^o$. Formally, the StyleGAN consists of a mapping function $h : \mathcal{Z} \to \mathcal{W}$ and a synthesis network $\tilde{g} : \mathcal{W} \to \mathcal{X}$. The mapping function takes a latent code z and outputs a style code w in an intermediate latent space $\mathcal{W}$. Then, the synthesis network takes the style code and produces a natural-looking image $\tilde{g}(w)$. We follow [41] and consider the extended latent space of StyleGAN. In [41], it has been shown that embedding images into the extended latent space is easier than $\mathcal{Z}$ or $\mathcal{W}$ space. Therefore, in the following, we consider $g : \mathcal{W}^+ \to \mathcal{X}$ as the generator function which approximates the image manifold for $\mathcal{D}_{tr}^o$.

In order to obtain images that are completely on-manifold, for each image x_i in $\mathcal{D}_{tr}^o$ and $\mathcal{D}_{te}^o$, we project onto the learned manifold by solving for its latent representation w_i [41]. We use a weighted combination of the Learned Perceptual Image Patch Similarity (LPIPS) [42] and L_1 loss to measure the closeness between $g(w)$ and x_i. LPIPS is shown to be a more suitable measure for perceptual similarity than conventional metrics, and its combination with L_1 or L_2 loss has been shown successful for inferring the latent representation of GANs. We adopt this strategy and solve for the latent representation by:

$$w_i = \arg\min_{w} \text{LPIPS}(g(w), x_i) + \|g(w) - x_i\|_1. \tag{7}$$

In summary, the resulting on-manifold training and test sets can be represented by: $\mathcal{D}_{tr} = \{(w_i, g(w_i), x_i, y_i)\}_{i=1}^{N}$, and $\mathcal{D}_{te} = \{(w_j, g(w_j), x_j, y_j)\}_{j=1}^{M}$, where $N = 69,480$ and $M = 7,200$. The total number of categories is 10. Notice that for OM-ImageNet, the underlying manifold information is exact, which is given by $\{g(w), w \in \mathcal{W}^+\}$. Sample on-manifold images $g(w_i)$ from OM-ImageNet are presented in Figure 2. On-manifold images in OM-ImageNet have diverse textures, object sizes, lightening, and poses, which is suitable for investigating the potential benefits of using manifold information in more general scenarios.
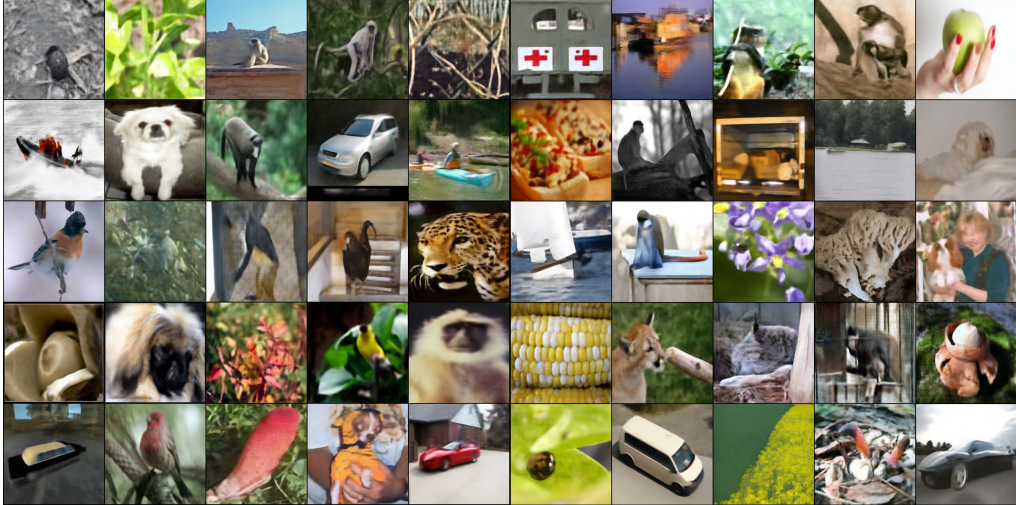
4

Figure 2: Sample images from the OM-ImageNet dataset. Unlike MNIST-like [38, 35, 36] or CelebA [37] datasets, images in OM-ImageNet have diverse textures. Moreover, the underlying manifold information for this dataset is *exact*.
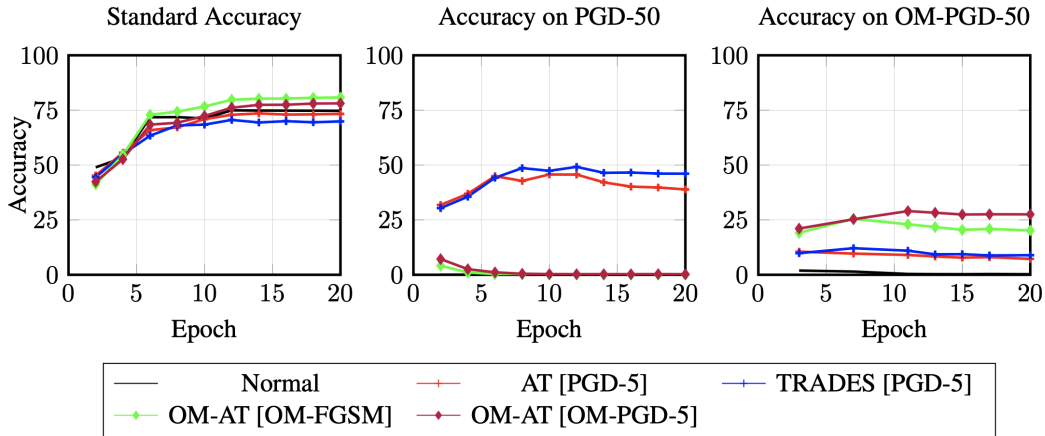

Figure 3: On-manifold adversarial training does not provide robustness to standard attacks. Standard adversarial training does not provide robustness to on-manifold attacks. Left: standard accuracy. Middle: classification accuracy when the trained models are attacked by PGD-50. Right: classification accuracy when the trained models are attacked by OM-PGD-50.

4   On-Manifold AT Cannot Defend Standard Attacks and Vice Versa

One issue we would like to investigate first is whether the manifold information alone can improve robustness. We use OM-ImageNet and train several ResNet-50 models to achieve standard L_∞ robustness at a radius of $\epsilon = 4/255$ (according to optimization (8)) or on-manifold robustness at a radius of $\eta = 0.02$ in the latent space (according to optimization (9)).

$$\min_\theta \sum_i \max_\delta \mathcal{L}(f_\theta(g(w_i) + \delta), y_{\text{true}}), \ \ s.t. \ \|\delta\|_\infty < \epsilon. \tag{8}$$

$$\min_\theta \sum_i \max_\lambda \mathcal{L}(f_\theta(g(w_i + \lambda)), y_{\text{true}}), \ \ s.t. \ \|\lambda\|_\infty < \eta. \tag{9}$$

During training, we use the PGD-5 threat model in the image space for (8), whereas for (9) we consider OM-FGSM and OM-PGD-5 as the threat models. For completeness, we also consider robust training using TRADES ($\beta = 6$) [43] in the image space using the PGD-5 threat model. All the

Table 1: Classification accuracy for PGD-50 and OM-PGD-50 attacks on OM-ImageNet test set.

Method	Standard	FGSM	PGD-50	MIA	Worst Case	OM-PGD-50
Normal Training	74.72%	2.59%	0.00%	0.00%	0.00%	0.26%
AT [PGD-5]	73.31%	48.02%	38.88%	39.21%	38.80%	7.23%
OM-AT [OM-FGSM]	80.77%	17.15%	0.03%	0.01%	0.01%	20.19%
OM-AT [OM-PGD-5]	78.10%	21.68%	0.25%	0.12%	0.10%	27.53%
DMAT [PGD-5, OM-PGD-5]	77.96%	49.12%	37.86%	37.65%	36.66%	20.53%

models are trained by the SGD optimizer with the cyclic learning rate scheduling strategy in [44], momentum 0.9, and weight decay 5×10^{-4} for a maximum of 20 epochs.

We evaluate the trained models using the PGD-50 and OM-PGD-50 attacks for multiple snapshots during training. The results are presented in Figure 3. We observe that (i) standard adversarial training leads to degraded standard accuracy while on-manifold adversarial training improves it (consistent with [24, 34]) and (ii) standard adversarial training does not provide robustness to on-manifold attacks (consistent with [27]). Interestingly, we also observe that (iii) on-manifold adversarial training does *not* provide robustness to L_∞ attacks since no out-of-manifold samples are realized during training, and (iv) standard adversarial training does not provide robustness to on-manifold attacks.

5 Proposed Method: Dual Manifold Adversarial Training

The fact that standard adversarial training and on-manifold adversarial training bring complimentary benefits to the model robustness motivates us to consider the following *dual manifold adversarial training (DMAT)* framework:

$$\min_\theta \sum_i \left\{ \max_{\delta \in \Delta} \mathcal{L}(f_\theta(g(w_i) + \delta), y_{\text{true}}) + \max_{\lambda \in \Lambda} \mathcal{L}(f_\theta(g(w_i + \lambda)), y_{\text{true}}) \right\}, \qquad (10)$$

where we are trying to solve for a classifier f_θ that is robust to both off-manifold perturbations (achieved by the first term) and on-manifold perturbations (achieved by the second term). The perturbation budgets Δ and Λ control the strengths of the threat models during training. For evaluation purposes, we consider PGD-5 and OM-PGD-5 as the standard and on-manifold threat models during training with the same perturbation budgets used by AT and OM-AT. To optimize (10), in each iteration, both standard and on-manifold adversarial examples are generated for the classifier f_θ, and f_θ is updated by the gradient descent method. The robust model is trained with the identical optimizer setting as in Section 4.

5.1 DMAT Improves Generalization and Robustness

Table 1 presents classification accuracies for different adversarial training methods against standard and on-manifold adversarial attacks. For standard adversarial attacks, we consider a set of adaptive attacks: FGSM, PGD-50 and the Momentum Iterative Attack (MIA) [45]. We also report the per-sample worst case accuracy, where each test sample will be viewed as mis-classified if one of the attacks fools the classifier. For on-manifold adversarial attacks, we consider OM-PGD-50. Compared to standard adversarial training, DMAT achieves improved generalization on normal samples, and significant boost for on-manifold robustness, with a slightly degraded robustness against PGD-50 attack (with L_∞ bound of $4/255$). Compared to on-manifold adversarial training (OM-AT [OM-FGSM] and OM-AT [OM-PGD-5]), since out-of-manifold samples are realized for DMAT, robustness against the PGD-50 attack is also significantly improved.

In Figure 4, we visualize PGD-50 and OM-PGD-50 adversarial examples crafted for the trained models. We can see that for the PGD-50 attack, stronger high-frequency perturbations (colored in red) are crafted for models trained by standard adversarial training and DMAT. For the OM-PGD-50 attack, manipulations in semantic-related regions need to be stronger in order to mislead models trained by on-manifold adversarial training and DMAT.
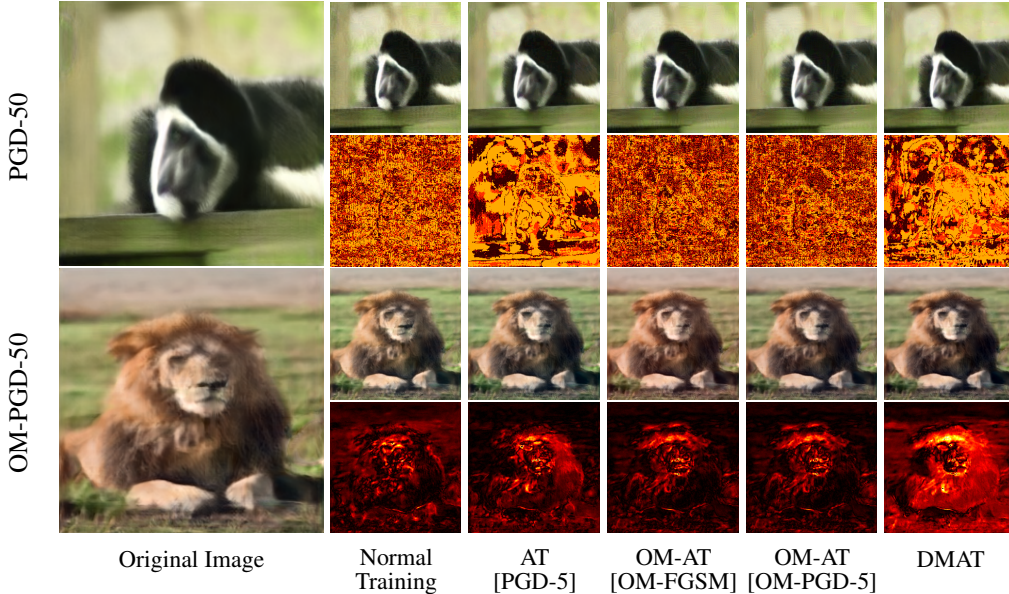
Figure 4: Examples of crafted adversarial examples with the corresponding difference images to the original images using PGD-50 (top) and OM-PGD-50 (bottom) attacks for different robustified models. Brighter colors indicate larger distortions. We can observe that the PGD-50 adversary causes stronger perturbations for classifiers trained with AT and DMAT, and the OM-PGD-50 adversary causes stronger perturbations for the classifier defended by DMAT. In these cases, the model trained by DMAT is more robust and requires stronger distortions to break.

5.2 DMAT Improves Robustness to Unseen Attacks

After demonstrating the improved robustness on known attacks brought by DMAT, we investigate whether DMAT improves robustness against novel attacks. We consider several perceptual attacks proposed in [26] including Fog, Snow, Gabor, Elastic, JPEG, L_2, and L_1 attacks, which apply global color shifts and image filtering to the normal images. Notice that we do not consider the extremely high attack strengths as in [26] since we focus on untargeted attacks. Results presented in Table 2 demonstrate that compared to standard adversarial training, DMAT is more robust against these attacks that are not seen during training. In Figure 5, we visualize the Fog, JPEG compression, and Snow adversarial examples for the trained models. These novel adversaries need to cause stronger distortions on DMAT than standard adversarial training and on-manifold adversarial training to mislead the corresponding classifiers.

Table 2: Classification accuracy against unseen attacks applied to OM-ImageNet test set.

Method	Fog	Snow	Elastic	Gabor	JPEG	L_2	L_1
Normal Training	0.03%	0.06%	1.20%	0.03%	0.00%	1.70%	0.00%
AT [PGD-5]	19.76%	46.39%	50.32%	50.43%	10.23%	41.98%	21.21%
OM-AT [OM-FGSM]	11.12%	13.82%	34.07%	1.50%	0.26%	2.27%	8.59%
OM-AT [OM-PGD-5]	22.39%	28.38%	48.74%	5.19%	0.49%	5.92%	14.67%
DMAT [PGD-5, OM-PGD-5] **(Ours)**	**31.78%**	**51.19%**	**56.09%**	**51.61%**	**14.31%**	**51.36%**	**29.68%**

5.3 TRADES for DMAT

The proposed DMAT framework is general and can be extended to other adversarial training approaches such as TRADES [43]. TRADES is one of the state-of-the-art methods that achieves better trade-off between standard accuracy and robustness compared to standard AT (3). We adopt TRADES in DMAT by considering the following loss function:

$$\min_{\theta} \sum_i \mathcal{L}(f_\theta(x_i), y_{true}) + \beta \max_{\delta} \mathcal{L}(f_\theta(x_i), f_\theta(x_i + \delta)) + \beta \max_{\lambda} \mathcal{L}(f_\theta(x_i), f_\theta(g(w_i + \lambda))), \quad (11)$$

Figure 5: Examples of crafted adversarial examples using the Fog attack (top row), the JPEG compression attack (middle row) and the snow attack (bottom row) for different robustified models. Brighter colors indicate larger absolute differences. We can observe that the classifier trained with DMAT is more robust and needs stronger distortions to break.

where $x_i = g(w_i)$. The first two terms in (11) are the original TRADES in the image space, and the third term is the counterpart in the latent space. To solve for the two maximization problems in (11), we use PGD-5 and OM-PGD-5 with the same parameter settings. Results are presented in Table 3.

Table 3: Classification accuracy against known (PGD-50 and OM-PGD-50) and unseen attacks applied to OM-ImageNet test set. Even for TRADES, the benefit of using manifold information can also be observed.

Method	Standard	PGD-50	OM-PGD-50	Fog	Snow	Elastic	Gabor	JPEG	L_2
Normal Training	74.72%	0.00%	0.26%	0.03%	0.06%	1.20%	0.03%	0.00%	1.70%
TRADES	69.88%	**46.06%**	8.92%	18.14%	**47.63%**	53.32%	**54.33%**	14.06%	46.36%
DMAT + TRADES	73.17%	42.57%	**26.82%**	**30.64%**	46.62%	**56.38%**	53.43%	**23.62%**	**55.09%**

5.4 Evaluations on Out-of-Manifold (Natural) Samples

In previous sections, we have considered adversaries crafting adversarial perturbations and applying them on samples in the On-Manifold ImageNet. However, we would also like to explore the scenario when the given natural images are out-of-manifold. Specifically, we evaluate the trained models by using $\{x_j\}_{j=1}^M$ as normal, and likely out-of-manifold images. Interestingly, from the results presented in Table 4, we observe that all adversarial training methods generalize well for out-of-manifold normal images, while normal training leads to degraded performance. Furthermore, consistent with the findings in previous sections, DMAT leads to comparable robustness with standard adversarial

training against PGD-50 attacks, and an improved robustness compared to standard adversarial training against unseen attacks. These results demonstrate a promising direction of using manifold information (exactly or approximately) to enhance the robustness of deep learning models.

Table 4: Generalization of the defended models to natural (out-of-manifold) images.

Method	Standard	PGD-50	Fog	Snow	Elastic	Gabor	JPEG	L_2	L_1
Normal Training	67.21%	0.00%	0.38%	0.35%	0.69%	0.04%	0.00%	1.26%	0.01%
AT [PGD-5]	71.08%	**37.32%**	23.28%	45.88%	46.72%	**46.17%**	9.00%	39.72%	21.21%
OM-AT [OM-FGSM]	**79.15%**	0.19%	23.41%	24.00%	33.53%	2.53 %	0.41%	3.70%	8.59%
OM-AT [OM-PGD-5]	73.88%	0.35%	32.34%	36.66%	46.50%	7.25%	0.52%	8.38%	14.67%
DMAT (Ours)	74.72%	34.63%	**36.25%**	**50.56%**	**54.14%**	45.39%	**13.29%**	**48.42%**	**29.68%**

6 Conclusion

In this paper, we investigate whether information about the underlying manifold of natural images can be leveraged to train deep learning models with improved robustness, in particular against unseen and novel attacks. For this purpose, we create the OM-ImageNet dataset, which consists of images with rich textures that are completely on-manifold. The manifold information is exact for OM-ImageNet. Using OM-ImageNet, we show that on-manifold AT cannot defend standard attacks and vice versa. The complimentary benefits of standard and on-manifold AT inspire us to propose dual manifold adversarial training (DMAT) where crafted adversarial examples both in image and latent spaces are used to robustify the underlying model. DMAT improves generalization and robustness to both L_p and non-L_p adversarial attacks. Also, similar improvements are achieved on (out-of-manifold) natural images. These results crystallize the use of the underlying manifold information of images to enhance the intrinsic robustness of the models, specially against novel adversarial attacks.

7 Broader Impact

Deep neural networks have been broadly applied to various fields because of their superior performance. However, their vulnerability to adversarial attacks makes general public worry, especially in some security-critical applications such as autonomous vehicle and medical diagnosis. Therefore, we need a method that makes neural networks robust to different attacks. In this work, we explore whether or not leveraging the underlying manifold information could enhance the robustness and generalization capability of neutral networks. We provide an affirmative answer to this question. With the proposed novel OM-ImageNet dataset, future works in this direction could be facilitated. The proposed method DMAT demonstrates a way to enhance both robustness and generalization to known and novel adversarial attacks.

We note that it is possible that future stronger attacks decrease the performance of the proposed defenses. This work should therefore be viewed as a necessary but not sufficient step towards understanding the role of generative image manifolds in the robustness of vision systems against a wide range of adversarial attacks. We anticipate more works on enhancing both robustness and generalization of deep neural networks to gain public confidence in deep learning systems.

References

[1] Alex Krizhevsky, Ilya Sutskever, and Geoffrey Hinton. Imagenet classification with deep convolutional neural networks. *Advances in Neural Information Processing Systems*, 25, 01 2012.

[2] Ross Girshick. Fast r-cnn. In *International Conference on Computer Vision (ICCV)*, 2015.

[3] G. Hinton, L. Deng, D. Yu, G. E. Dahl, A. Mohamed, N. Jaitly, A. Senior, V. Vanhoucke, P. Nguyen, T. N. Sainath, and B. Kingsbury. Deep neural networks for acoustic modeling in speech recognition: The shared views of four research groups. *IEEE Signal Processing Magazine*, 29(6):82–97, 2012.

[4] Christian Szegedy, Wojciech Zaremba, Ilya Sutskever, Joan Bruna, Dumitru Erhan, Ian Goodfellow, and Rob Fergus. Intriguing properties of neural networks. In *International Conference on Learning Representations*, 2014.

[5] Ian J. Goodfellow, Jonathon Shlens, and Christian Szegedy. Explaining and harnessing adversarial examples. *International Conference on Learning Representations*, 2015.

[6] Nicholas Carlini and David Wagner. Towards evaluating the robustness of neural networks. In *IEEE Symposium on Security and Srivacy (SP)*, pages 39–57. IEEE, 2017.

[7] Anish Athalye, Nicholas Carlini, and David Wagner. Obfuscated gradients give a false sense of security: Circumventing defenses to adversarial examples. In *International Conference on Machine Learning*, pages 274–283, 2018.

[8] Alhussein Fawzi, Hamza Fawzi, and Omar Fawzi. Adversarial vulnerability for any classifier. In *Advances in Neural Information Processing Systems*, 2018.

[9] Anish Athalye, Logan Engstrom, Andrew Ilyas, and Kevin Kwok. Synthesizing robust adversarial examples. In *International Conference on Machine Learning*, pages 284–293, 2018.

[10] Chang Xiao, Peilin Zhong, and Changxi Zheng. Resisting adversarial attacks by k-winners-take-all. *arXiv preprint arXiv:1905.10510*, 2019.

[11] Kevin Roth, Yannic Kilcher, and Thomas Hofmann. The odds are odd: A statistical test for detecting adversarial examples. In *International Conference on Machine Learning*, pages 5498–5507, 2019.

[12] Tianyu Pang, Kun Xu, and Jun Zhu. Mixup inference: Better exploiting mixup to defend adversarial attacks. In *International Conference on Learning Representations*, 2019.

[13] Pouya Samangouei, Maya Kabkab, and Rama Chellappa. Defense-GAN: Protecting classifiers against adversarial attacks using generative models. *arXiv preprint arXiv:1805.06605*, 2018.

[14] Eric Wong and Zico Kolter. Provable defenses against adversarial examples via the convex outer adversarial polytope. In *International Conference on Machine Learning*, pages 5286–5295, 2018.

[15] Aditi Raghunathan, Jacob Steinhardt, and Percy S Liang. Semidefinite relaxations for certifying robustness to adversarial examples. In *Advances in Neural Information Processing Systems*, pages 10877–10887, 2018.

[16] Jeremy Cohen, Elan Rosenfeld, and Zico Kolter. Certified adversarial robustness via randomized smoothing. In *International Conference on Machine Learning*, pages 1310–1320, 2019.

[17] Alexander Levine and Soheil Feizi. Wasserstein smoothing: Certified robustness against wasserstein adversarial attacks. In *International Conference on Artificial Intelligence and Statistics*, 2020.

[18] Ping-Yeh Chiang, Renkun Ni, Ahmed Abdelkader, Chen Zhu, Christoph Studor, and Tom Goldstein. Certified defenses for adversarial patches. *arXiv preprint arXiv:2003.06693*, 2020.

[19] Alexander Levine and Soheil Feizi. Robustness certificates for sparse adversarial attacks by randomized ablation. *Association for the Advancement of Artificial Intelligence (AAAI)*, 2020.

[20] Xingjun Ma, Bo Li, Yisen Wang, Sarah M Erfani, Sudanthi Wijewickrema, Grant Schoenebeck, Dawn Song, Michael E Houle, and James Bailey. Characterizing adversarial subspaces using local intrinsic dimensionality. *arXiv preprint arXiv:1801.02613*, 2018.

[21] Dongyu Meng and Hao Chen. Magnet: a two-pronged defense against adversarial examples. In *Proceedings of the 2017 ACM SIGSAC Conference on Computer and Communications Security*, pages 135–147, 2017.

[22] Weilin Xu, David Evans, and Yanjun Qi. Feature squeezing: Detecting adversarial examples in deep neural networks. *arXiv preprint arXiv:1704.01155*, 2017.

[23] Aleksander Madry, Aleksandar Makelov, Ludwig Schmidt, Dimitris Tsipras, and Adrian Vladu. Towards deep learning models resistant to adversarial attacks. *arXiv preprint arXiv:1706.06083*, 2017.

[24] Dimitris Tsipras, Shibani Santurkar, Logan Engstrom, Alexander Turner, and Aleksander Madry. Robustness may be at odds with accuracy. In *International Conference on Learning Representations (ICLR)*, 2019.

[25] Cassidy Laidlaw and Soheil Feizi. Functional adversarial attacks. In *Advances in Neural Information Processing Systems (NeurIPS)*, 2019.

[26] Daniel Kang, Yi Sun, Dan Hendrycks, Tom Brown, and Jacob Steinhardt. Testing robustness against unforeseen adversaries. *arXiv preprint arXiv:1908.08016*, 2019.

[27] Yang Song, Rui Shu, Nate Kushman, and Stefano Ermon. Constructing unrestricted adversarial examples with generative models. In *Advances in Neural Information Processing Systems (NeurIPS)*, 2018.

[28] Omid Poursaeed, Tianxing Jiang, Harry Yang, Serge Belongie, and Ser-Nam Lim. Fine-grained synthesis of unrestricted adversarial examples, 2019.

[29] Andrew Brock, Jeff Donahue, and Karen Simonyan. Large scale GAN training for high fidelity natural image synthesis. In *International Conference on Learning Representations*, 2019.

[30] Tero Karras, Samuli Laine, Miika Aittala, Janne Hellsten, Jaakko Lehtinen, and Timo Aila. Analyzing and improving the image quality of StyleGAN. *arXiv preprint arXiv:1912.04958*, 2019.

[31] Oriol Vinyals Ali Razavi, Aaron van den Oord. Generating diverse high-fidelity images with vq-vae-2. *arXiv preprint arXiv:1906.00446*, 2019.

[32] Andrew Ilyas, Shibani Santurkar, Dimitris Tsipras, Logan Engstrom, Brandon Tran, and Aleksander Madry. Adversarial examples are not bugs, they are features. In *Advances in Neural Information Processing Systems*, 2019.

[33] Ajil Jalal, Andrew Ilyas, Constantinos Daskalakis, and Alexandros G Dimakis. The robust manifold defense: Adversarial training using generative models. *arXiv preprint arXiv:1712.09196*, 2017.

[34] David Stutz, Matthias Hein, and Bernt Schiele. Disentangling adversarial robustness and generalization. In *The IEEE Conference on Computer Vision and Pattern Recognition (CVPR)*, June 2019.

[35] Gregory Cohen, Saeed Afshar, Jonathan Tapson, and André van Schaik. Emnist: an extension of mnist to handwritten letters. *arXiv preprint arXiv:1702.05373*, 2017.

[36] Han Xiao, Kashif Rasul, and Roland Vollgraf. Fashion-mnist: a novel image dataset for benchmarking machine learning algorithms. *arXiv preprint arXiv:1708.07747*, 2017.

[37] Ziwei Liu, Ping Luo, Xiaogang Wang, and Xiaoou Tang. Deep learning face attributes in the wild. In *International Conference on Computer Vision (ICCV)*, December 2015.

[38] Y. Lecun, L. Bottou, Y. Bengio, and P. Haffner. Gradient-based learning applied to document recognition. *Proceedings of the IEEE*, 86(11):2278–2324, 1998.

[39] Logan Engstrom, Andrew Ilyas, Shibani Santurkar, and Dimitris Tsipras. Robustness (python library), 2019.

[40] Tero Karras, Samuli Laine, and Timo Aila. A style-based generator architecture for generative adversarial networks. In *The IEEE Conference on Computer Vision and Pattern Recognition (CVPR)*, June 2019.

[41] Rameen Abdal, Yipeng Qin, and Peter Wonka. Image2StyleGAN: How to embed images into the StyleGAN latent space? In *The IEEE International Conference on Computer Vision (ICCV)*, October 2019.

[42] Richard Zhang, Phillip Isola, Alexei A Efros, Eli Shechtman, and Oliver Wang. The unreasonable effectiveness of deep features as a perceptual metric. In *Proceedings of the IEEE Conference on Computer Vision and Pattern Recognition*, pages 586–595, 2018.

[43] Hongyang Zhang, Yaodong Yu, Jiantao Jiao, Eric P. Xing, Laurent El Ghaoui, and Michael I. Jordan. Theoretically principled trade-off between robustness and accuracy. In *Advances in Neural Information Processing Systems*, 2019.

[44] Eric Wong, Leslie Rice, and J. Zico Kolter. Fast is better than free: Revisiting adversarial training. In *International Conference on Learning Representations*, 2020.

[45] Yinpeng Dong, Fangzhou Liao, Tianyu Pang, Hang Su, Jun Zhu, Xiaolin Hu, and Jianguo Li. Boosting adversarial attacks with momentum. In *The IEEE Conference on Computer Vision and Pattern Recognition (CVPR)*, 2018.